

ON SOLUTIONS TO PROBLEMS OF BOTTOM DEFORMATIONS WITH ALLOWANCE FOR THEIR SELF-SIMILARITY

A. G. Petrov,¹ I. I. Potapov,² and A. S. Epikhin³

Translated from *Gidrotekhnicheskoe Stroitel'svo*, No. 6, June 2024, pp. 16 – 22. DOI: 10.34831/EP.2024.71.86.003

A method for establishing a self-similar dependence of the bottom surface on time and spatial coordinate is proposed. The mean bottom tangential stresses are determined for a series of self-similar shapes of the bottom to then calculate the rates of change in the lengths and amplitudes of the bottom waves. Comparison with experimental data and numerical solutions shows that the error of the solution does not exceed several percent and that the computation time is shorter by a factor of 25 to 30 than that of conventional evolutionary computation.

Keywords: self-similarity; bottom waves; channel process; erosion; OpenFOAM.

A conventional approach to the study of bottom deformations induced by the hydrodynamic flow employs nonstationary channel models [1], which involves a high computational burden [2]. Since the solutions of such problems are used in many applied projects (pipeline laying on the river bottom [3 – 5], bottom deformation downstream of hydraulic projects [6 – 8], effect of ship propulsors on the bottom [9], etc.), it is of high interest to reduce the computation time using the observed self-similarity of bottom deformations.

We will analyze the possibility of using the self-similar behavior of bottom deformation to substantially reduce the time of computing the channel process evolving in a self-similar approximation.

Self-similar bottom erosion. Experimental data on the erosion of the river bottom under the action of the hydrodynamic flow [3 – 9] show that these processes are self-similar. The experimental curves in Fig. 1 demonstrate that the bottom surface at any time point can be represented as follows:

$$\frac{\zeta}{\zeta_0} = \frac{\zeta(t, x)}{\zeta_0(t)} = \begin{cases} -\sin\left(2\pi \frac{qx}{\zeta_0(t)}\right), & \frac{qx}{\zeta_0(t)} \in (0, 1) \\ 0; \frac{qx}{\zeta_0} & (t_0 \notin (0, 1)) \end{cases} \quad (1.1)$$

¹ Ishlinsky Institute for Problems of Mechanics, Russian Academy of Sciences, Moscow, Russia; e-mail: petrovipmech@gmail.com

² Khabarovsk Federal Research Center, Computing Center, Far East Branch of the Russian Academy of Sciences, Khabarovsk, Russia; e-mail: potapov2i@gmail.com

³ Ivannikov Institute for System Programming, Russian Academy of Sciences, Moscow, Russia; e-mail: andreypikhin@ispras.ru

$$q = \frac{\zeta_0(t)}{\zeta(t)}. \quad (1.2)$$

Physically, the quantity q is the steepness of a bottom wave and is considered constant according to experimental data on various channel processes. For example, $q = \zeta_0(t)/\lambda(t) = 0.08$ for the evolution of a bottom surface under a pipe on the river bottom (Fig. 1a [5]). Another example of the evolution of the bottom surface under the action of a plane bottom jet (submerged sluice gate flow) is shown in Fig. 1b [7]. It can be seen that at six different time points, the bottom surface remains sinusoidal, the length and amplitude of the bottom wave change, and their ratio remains constant.

The self-similar sinusoidal modes are shown by solid lines in Fig. 1. The time dependence of the wave amplitude $\zeta_0 = \zeta_0(t)$ and the wave length $\lambda = \lambda(t)$ is approximated by the following power functions:

$$\lambda = \alpha t^\beta, \quad \zeta_0 = q\alpha t^\beta. \quad (0.3)$$

For example, $\alpha = 70$ and $\beta = 1/8$ for the self-similar bottom modes in Fig. 1a.

Mathematical problem statement. The evolution of the bottom level ζ is described using the law of conservation of sediment mass (Exner equation):

$$(1 - \epsilon) \frac{\partial \zeta}{\partial t} + \frac{\partial G}{\partial x} = 0, \quad (3.1)$$

where G is the volume flow rate of transported sediments in the active near-bottom layer; ϵ is the porosity of sediment.

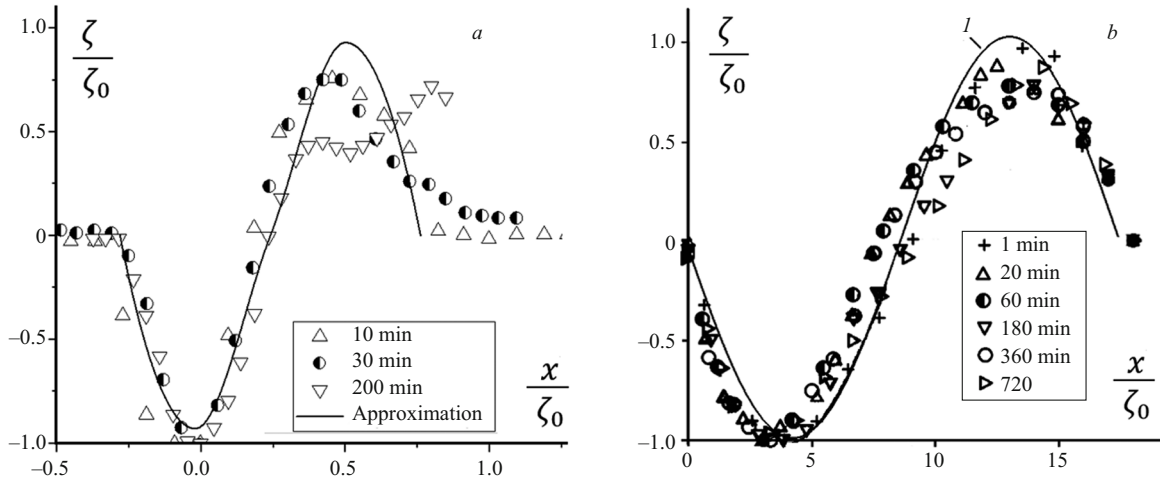


Fig. 1. Evolution of bottom surface: *a*, under a pipe on river bottom [5]; *b*, under the action of a plane bottom jet according to [7]; *1*, sinusoidal approximation.

The following theoretical dependence is used to close the equation:

$$G = G_0 \frac{(T - T_c)^{3/2} X}{1 + \Gamma}, \quad (3.2)$$

$$\Gamma = \frac{1}{\tan \phi} \frac{\partial \zeta}{\partial x}, \quad T_c = T_0(1 + \Gamma),$$

$$T_0 = \frac{9}{8} \frac{\kappa^2 \tan \phi}{c_x} G_0 = \frac{g_0}{g(\rho_s - \rho_w) \sqrt{\rho_w}},$$

$$g_0 = \frac{4}{3} \frac{1}{\kappa \tan \phi},$$

where T_c is the critical bottom shear stress; T_0 is the critical stress on the flat bottom; $X = X(T - T_c)$ is the Heaviside function.

The theoretical dependence (3.2) was confirmed by all well-known and reliable experimental data. Equations (3.2) and (3.1) and the hydrodynamic equations constitute a closed, yet very complex system of equations describing the evolution of the bottom surface under the action of various hydrodynamic factors such as flow under pipe, near-bottom jet, etc. The self-similar geometry of a bottom wave can be used to describe its evolution, which reduces the computation time by almost two orders of magnitude.

Stress distribution over bottom surface. The self-similar solution (2.1) can be used to find the stress distribution over the bottom surface. To this end, we substitute it into the Exner equation. The time derivative of the function $\zeta = \zeta(t, x)$ is given by

$$\frac{\partial \zeta}{\partial t} = q\lambda \left(-\sin\left(\frac{2\pi x}{\lambda}\right) + \frac{2\pi x}{\lambda} \cos\left(\frac{2\pi x}{\lambda}\right) \right), \quad \dot{\lambda} = \frac{\partial \lambda}{\partial t}.$$

Let us integrate the Exner equation with respect to x :

$$(1 - \epsilon) \int_0^x \frac{\partial \zeta}{\partial t} dx + G(t, x) = G(0).$$

Using the replacement

$$\int_0^x \frac{\partial \zeta}{\partial t} dx = q\lambda \left(x \sin\left(\frac{2\pi x}{\lambda}\right) - \frac{\lambda}{\pi} \left(1 - \cos\left(\frac{2\pi x}{\lambda}\right) \right) \right) = -\frac{q\lambda \dot{\lambda}}{2\pi} \Phi,$$

we get

$$G(t, x) = (1 - \epsilon) \frac{q\lambda \dot{\lambda}}{2\pi} \Phi(\xi),$$

$$\Phi = 2 - 2 \cos \zeta - \zeta \sin \zeta, \quad \zeta = 2\pi x / \lambda.$$

Assuming that the sediment transport rate $G(0)$ is equal to zero and using (3.2), we obtain the equation describing the distribution of the stress T over the bottom surface:

$$G_0 \frac{(T - T_c)^{3/2} X}{1 + \Gamma} = (1 - \epsilon) \frac{q\lambda \dot{\lambda}}{2\pi} \Phi,$$

Resolving this equation for T yields

$$\frac{T}{T_0} = 1 + \Gamma + ((1 + \Gamma)\Phi\Lambda)^{2/3}, \quad (4.1)$$

$$\Gamma = \frac{1}{\tan \phi} \frac{\partial \zeta}{\partial x} = -\frac{2\pi q}{\tan \phi} \cos \xi, \quad \Lambda = (1 - \epsilon) \frac{q\lambda \dot{\lambda}}{2\pi G_0 T_0^{3/2}}.$$

The graphs of the functions Φ and Γ appearing in (4.1) are shown in Fig. 2.

Equation (4.1) can be used to relate the mean stress on the bottom wave and the function $\Lambda(t)$:

$$\frac{\bar{T}}{T} = \frac{1}{2\pi} \int_0^{2\pi} \frac{T}{T_0} d\xi = 1 + C\Lambda^{3/2},$$

$$C = \frac{1}{2\pi} \int_0^{2\pi} \left(1 - \frac{2\pi q}{\tan \phi} \cos \xi\right)^{3/2} \Phi^{3/2} d\xi.$$

As the factor $2\pi q/\tan \phi$ changes from 0.4 to 0.8, the coefficient C changes insignificantly from 1.97 to 2.01. Therefore, we can set

$$\frac{\bar{T}}{T_0} = \frac{1}{2\pi} \int_0^{2\pi} \frac{T}{T_0} d\xi = 1 + 2\Lambda^{2/3}. \quad (4.2)$$

Using (4.1) to resolve this equation for λ , we obtain the differential relation

$$\dot{\lambda} = \frac{K}{\lambda} \left(\frac{\bar{T}}{T_0} - 1\right)^{3/2}, \quad K = \frac{\pi G_0 T_0^{3/2}}{\sqrt{2}(1-\epsilon)q}. \quad (4.3)$$

Algorithm for computing the evolution of a self-similar bottom wave. We propose the following algorithm to analyze the evolution of a self-similar bottom wave (2.3) using Eq. (4.3). Consider a set of bottom waves (2.1) with lengths λ_i , $i = 1, \dots, N$. The stress distribution over the uniform mesh T_{ij} , $j = 1, \dots, M$, of each bottom wave λ_i is found from the solution of the hydrodynamic equations. These values and the formula

$$\frac{\bar{T}_i}{T_0} = \frac{1}{MT_0} \sum_{k=1}^M T_{ik}$$

are used to calculate the values of \bar{T}_i / T_0 , and the differential relation is used to find a table of values of the derivatives $\dot{\lambda}_i$. The tabulated values are approximated as

$$\dot{\lambda} = A\lambda^{-n}. \quad (5.1)$$

The constants A and n are determined by the least-squares method. Minimizing the function

$$F = \sum_{i=1}^N (\ln \lambda_i - \ln A + n \ln \lambda_i)^2$$

we obtain a system of two linear equations for the unknowns $\ln A$ and n :

$$\sum_{i=1}^n (\ln \dot{\lambda}_i - \ln A + n \ln \lambda_i) = 0,$$

$$\sum_{i=1}^n (\ln \lambda_i - \ln A + n \ln \lambda_i) \ln \lambda_i = 0. \quad (5.2)$$

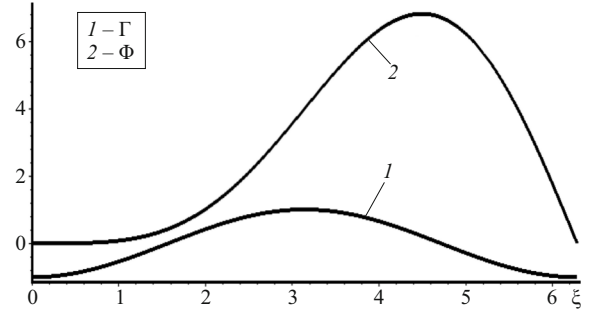


Fig. 2. Graphs of the functions Φ and Γ .

Equation (5.1) has the exact solution.

$$\lambda = [(1+n)A]^{1/(1+n)} t^{1/(1+n)}. \quad (5.3)$$

Substituting the values of A and n found from the system of equations into it yields the function λ . This approach allows reducing the computation time substantially.

Discussion of the results. We used OpenFOAM open-source software for numerical calculation of stresses on sinusoidal bottom. We considered a water flow (velocity = 0.4 m/sec) past a cylinder (diameter $D = 0.1$ m) with different shapes of the bottom surface and determined the stresses on the bottom surface for sinusoidal modes with wave lengths $\kappa = 0.125, 0.2, 0.3, 0.4, 0.6$ and steepness $q = a/\lambda = 0.08$. Figure 3 shows the problem statement (a) and the calculated results for the flow past a cylinder over bottom waves with 3D wavelength (b) and 6D wavelength (c).

The data for bottom sand in SI units: sand grain diameter $d = 0.00035$, porosity $\phi = 0.35$, von Kármán constant $\kappa = 0.25$, the resistance coefficient of sand grains $cx = 0.55$, critical friction angle $\tan \phi = 0.5$, sand density $\rho_s = 2650$, water density $\rho_w = 1000$. The stress at infinity is equal to 0.36. Transported sediments are absent.

After numerical simulation for five values of the wavelength λ and wave steepness $q = 0.08$, we determined the mean stress \bar{T} and the rate of change in wavelength $d\lambda/dt$, their values being summarized in Table 1.

Using the system of equations (5.2) and the least-squares method, we found the coefficients of the interpolation function: $\dot{\lambda} = A\lambda^{-n}$, $\ln A = -12.47$, $n = 3.42$. Figure 4a compares the interpolation curve $\dot{\lambda} = A\lambda^{-n}$ and the data points (red circles) from Table 1. Substituting the found values of A and n

TABLE 1

λ	a	\bar{T}	$d\lambda/dt$
1.25D	0.1	0.99	0.00355
2D	0.16	0.84	0.00147
3D	0.24	0.56	0.000262
4D	0.32	0.46	0.0000686
6D	0.48	0.42	0.0000209

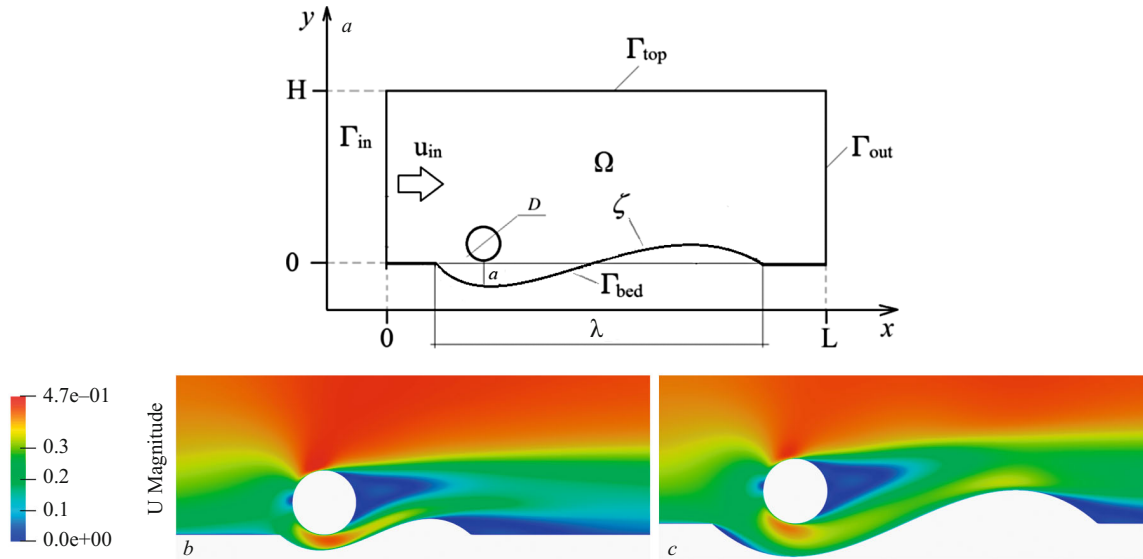


Fig. 3. Flow-past-cylinder problem statement: a , computational domain: Γ_{in} is the input boundary, Γ_{out} is the output boundary, Γ_{bed} is the bottom surface, Γ_{top} is the upper boundary; solution for flow past a cylinder over bottom waves; b , $3D$ wavelength; c , $6D$ wavelength.

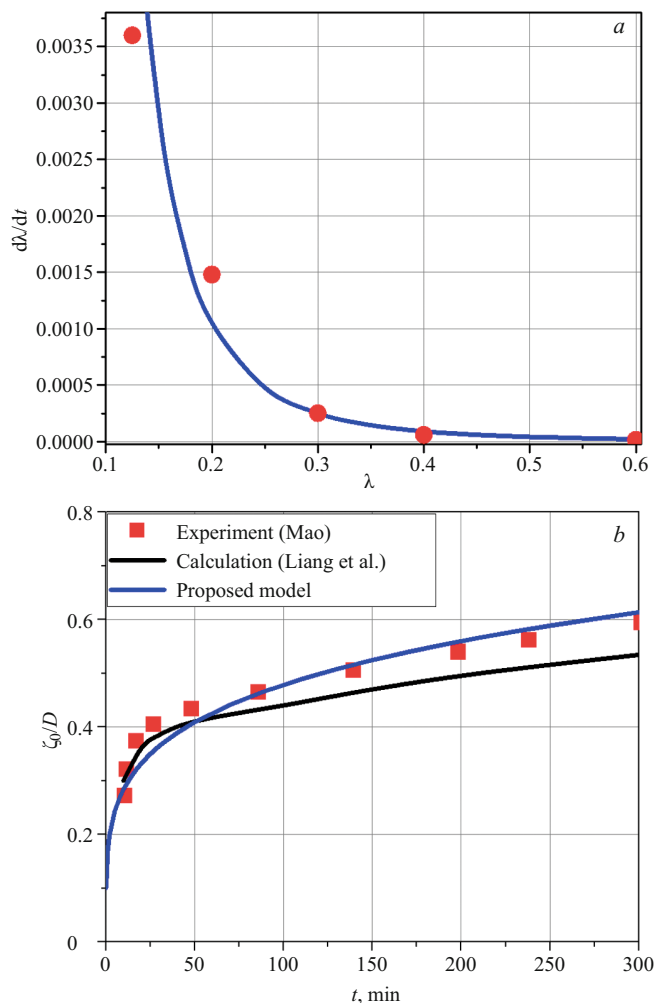


Fig. 4. Comparison of results: a , calculated data points with power approximation; b , calculation [10] (black curve), experimental data [5] (red squares), proposed model (blue curve).

into solution (5.3), we obtain the relation $\lambda = 0.0834t^{0.226}$ (where t is measured in seconds) or $\lambda = 0.211t^{0.226}$ (where t is measured in minutes) represented by the solid curve $\zeta_0/D = q\lambda/D$ in Fig. 4b, in comparison with the experimental data [5] and the calculated results for continuous erosion of the bottom surface and the deformation of the mesh [10].

The other problem [7] was a flow past a sinusoidal bottom shaped by a plane bottom jet from under a sluice gate. The design model of the problem is shown in Fig. 5a. The input parameters were: gate opening height $h = 0.015$ m; length of stable bottom section $l = 0.4$ m; water flow velocity under the gate $u_{in} = 1.21$ m/sec; flow depth in tailwater $H = 0.162$ m; total channel length $L = 6$ m. We calculated the stresses on the bottom surface for sinusoidal modes with wavelengths $\lambda_i = 0.4, 0.9, 1.03, 1.17, 1.36$ m and steepness $q = 0.054$. Figure 5 shows the problem statement (a) and the calculated results for the flow over bottom waves with wavelength λ_1 (b) and wavelength λ_4 (c).

The data for bottom sand in SI units: $d = 0.0008$, $\kappa = 0.23$, $c_x = 0.64$, $\tan \phi = 0.5$, $\rho_s = 2650$, $\rho_w = 1000$, $\phi = 0.35$. There are no transported sediments at the exit from the channel.

After numerical simulation for five values of the wavelength λ and wave steepness $q = 0.054$, we determined the mean stress T and the rate of change in wavelength $d\lambda/dt$, their values being summarized in Table 2.

As in the previous example, the coefficients A and n of the interpolation function were determined by the least-squares method: $A = 0.0000611$, $n = 4.333$. Substituting the found values of A and n into formula (5.3), we obtain the function whose graph is shown in Fig. 6 by a solid line and compared with experimental data (red symbols) [7].

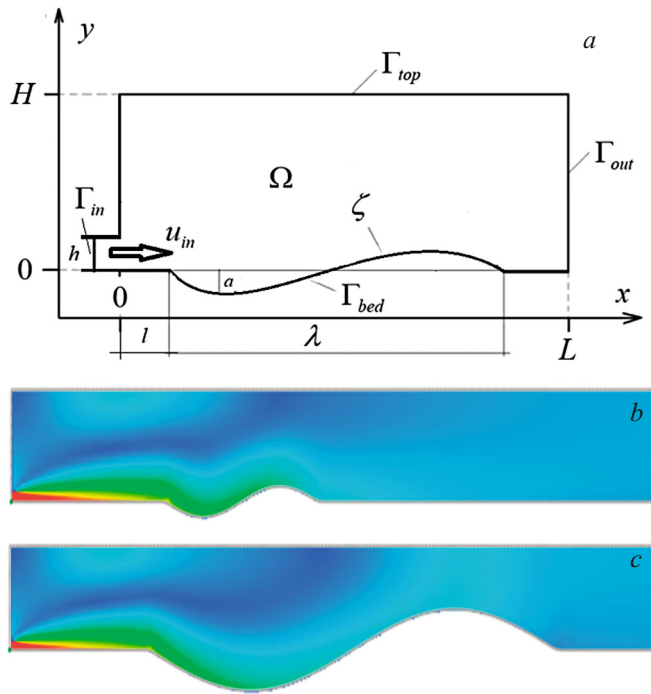


Fig. 5. Problem statement for flow past bottom wave: *a*, computational domain, Γ_{in} is the input boundary, Γ_{out} is the output boundary, Γ_{bed} is the bottom surface, Γ_{top} is the upper boundary; *b*, modes of bottom surface and calculated results for flow past bottom waves; *c*, wavelength $\lambda_1 = 0.4$ m; *d*, wavelength $\lambda_4 = 1.17$ m.

It can be seen that the numerical and experiment data are in good agreement with the theoretical model. The error of calculated ζ_0/ζ_{max} does not exceed ten percent.

Figures 4 and 6 also demonstrate satisfactory agreement between the theoretical model and the experimental data. The error of calculated ζ_0/ζ_{max} does not exceed several percent. The numerical simulation of hydrodynamics with allowance for erosion takes 8 h. The determination of the stresses for five cases and the solution of the problem by the algorithm proposed took about 15 min, i.e., the proposed approach allows us to reduce the computation time by 97%.

CONCLUSIONS

1. A mathematical model and a method of analyzing local erosion considering its self-similar evolutionary behavior have been proposed.
2. The method has been tested by solving two problems: local bottom erosion under a pipe and local bottom erosion by a jet from under a sluice gate. It has been shown that the self-similar behavior of bottom deformation allows an acceptable assessment of the bottom erosion depth in a time that is almost two orders of magnitude shorter than the time of numerical evolutionary simulation.
3. It is important that the proposed model, as well as other channel models, depends on numerical values of bot-

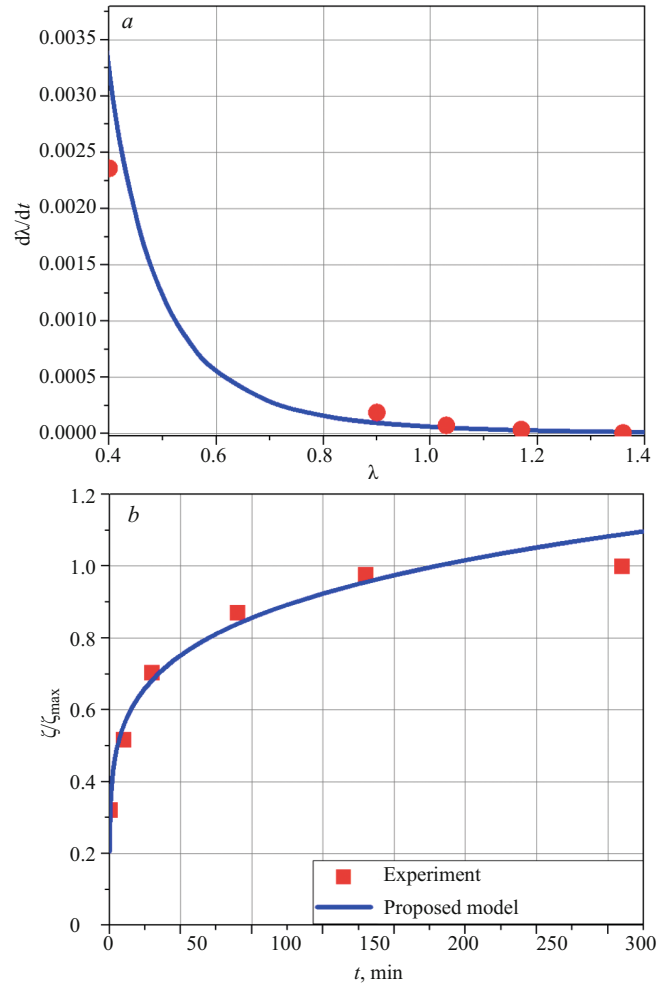


Fig. 6. Comparison of calculated results and experimental data [7] (red symbols), the proposed model (black curve).

tom stresses which are directly dependent on the turbulence model and its coefficients, the implementation of wall functions, and the mesh. Therefore, a wrong choice of a model for calculation of the bottom stresses may increase the error of calculation.

Compliance with ethical standards

Authors' contribution. The authors conducted the theoretical and numerical analyses, generalized the results, and wrote the manuscript, are copyright holders and responsible

TABLE 2

λ	a	\bar{T}	dx/dt
0.4	0.1	1.3483	0.002358
0.9	0.16	0.8332	0.0001886
1.03	0.24	0.7338	0.0000742
1.17	0.32	0.6878	0.000036257
1.36	0.48	0.6276	0.000007029

for plagiarism. All the authors contributed equally to the preparation of the publication.

Conflict of interest. The authors declare that they have no conflict of interest.

Funding. The study was sponsored by the Russian Science Foundation (grant No. 23-71-10091).

REFERENCES

1. A. G. Petrov and I. I. Potapov, *Selected Sections of Channel Dynamics* [in Russian], URSS, Moscow (2019).
2. V. V. Belikov, A. I. Aleksyuk, and E. S. Vasil'ev, *Numerical Simulation of Dam-Break Waves* [in Russian], RAN, Moscow (2023).
3. S. Paskin, *The Self-Burial of Seabed Pipelines. Doctoral Thesis*, London (1993).
4. S. Dey and N. P. Singh, "Clear-water scour below underwater pipelines under steady flow," *J. Hydr. Eng.*, **134**(5), 588 – 600 (2008).
5. Y. Mao, *The Interaction Between a Pipeline and an Erodible Bed. Ph.D. Thesis*, Technical University of Denmark, Lyngby, Denmark (1986).
6. S. S. Chatterjee, S. N. Ghosh, and M. Chatterjee, "Local scour due to submerged horizontal jet," *J. Hydr. Eng.*, **120**(8), 937 – 991 (1994).
7. S. Dey and A. Sarkar, "Scour downstream of an apron due to submerged horizontal jets," *J. Hydr. Eng.*, **132**(3), 246 – 257 (2006).
8. M. Aamir and Z. Ahmad, "Hydraulics of submerged jets causing scour downstream of a rough rigid apron," in: *Proc. of the 14th Int. Symp. on River Sedimentation (September 16 – 19, 2019, Chengdu, China)*, Chengdu (2019), pp. 1 – 10.
9. H. Samma, K. Amir, M. Rostam-Abadi, et al., "Numerical simulation of scour and flow field over movable bed induced by a submerged wall jet," *J. Hydroinformatics*, **22**(10), 386 – 401 (2020); DOI: 10.2166/hydro.2020.091
10. D. Liang, J. Huang, J. Zhang, et al., "Three-dimensional simulations of scour around pipelines of finite lengths," *J. Marine Sci. Eng.*, **10**(1), 106 (2022); doi: 10.3390/jmse10010106.